Bound electron *g*-factor measurement by double-resonance spectroscopy on a fine-structure transition[1]

David von Lindenfels, Nicolaas P.M. Brantjes, Gerhard Birkl, Wolfgang Quint, Vladimir M. Shabaev, and Manuel Vogel

Abstract: Precise determination of bound-electron *g*-factors in highly charged ions provides stringent tests for state of the art theoretical calculations. The scope reaches from relativistic electron-correlation effects on the one hand to bound-state QED terms on the other. Besides, the investigation can contribute to the determination of the fine-structure constant α. In a first approach with boron-like ions of spinless nuclei (e.g., $^{40}Ar^{13+}$ and $^{40}Ca^{15+}$), we will excite the $2^2P_{1/2}-2^2P_{3/2}$ fine-structure transition with laser radiation and probe microwave transitions between Zeeman sublevels. From this laser-microwave double-resonance technique the *g*-factor can be determined on a ppb level of accuracy. We have prepared a cryogenic trap assembly with a creation trap and a spectroscopy trap — a half-open compensated cylindrical Penning trap. Argon gas will be injected through a remotely controlled valve, working at cryogenic temperature and in the field of a superconducting magnet. Ions are produced by electron impact ionization and transferred to the spectroscopy trap. In the future, the trap will be connected to the HITRAP facility at GSI, and the method will be applied to hyperfine-structure transitions of hydrogen-like heavy ions to measure electronic and nuclear magnetic moments. We present important techniques employed in the experiment.

PACS Nos: 32.10.Dk, 32.10.Fn, 32.30.–r, 32.60.+i, 37.10.Ty, 42.62.Fi

Résumé : La mesure précise du facteur de Landé d'un électron lié offre la possibilité de tester de façon rigoureuse les dernières avancées théoriques. Ces dernières peuvent s'étendre des effets relativistes dans les corrélations électroniques, aux termes d'EDQ d'état lié. Par ailleurs, de tels investigations peuvent contribuer à la détermination de la constante de structure fine, α. Dans une première partie, nous décrirons l'excitation de la transition de structure fine $2^2P_{1/2}-2^2P_{3/2}$ d'ions boreoides sans spin nucléaire (e.g., argon $^{40}Ar^{13+}$ et calcium $^{40}Ca^{15+}$) par radiation laser, puis nous présenterons la mesure des transitions micro-ondes entre les sous-niveaux Zeeman. Grâce à cette technique de résonance double par laser et micro-ondes, le facteur de Landé peut être déterminé à un niveau de précision ppb. Nous avons préparé un montage de piège cryogénique comprenant un piège-création et un piège spectroscopique. Le gaz d'argon est injecté par l'intermédiaire d'une valve contrôlable à distance portée à des températures cryogéniques et dans le champs d'un aimant supraconducteur. Les ions sont produits par ionisation due à l'impact des électrons et transférés au piège spectroscopique. Dans le futur, le piège sera connecté au montage HITRAP, du laboratoire GSI-Darmstadt, et la méthode sera appliquée aux transitions hyperfines d'ions lourds hydrogenoides afin de mesurer les moments magnétiques électroniques et nucléaires. Nous présentons dans la suite des techniques importantes de l'expérience.

Received 13 July 2010. Accepted 30 August 2010. Published on the NRC Research Press Web site at cjp.nrc.ca on 21 December 2010.

D. von Lindenfels,[2] N.P.M. Brantjes, and W. Quint. GSI Helmholtzzentrum für Schwerionenforschung, Planckstr. 1, D-64291 Darmstadt, Germany.
G. Birkl. Institut für Angewandte Physik, TU Darmstadt, Schlossgartenstrasse 7, D-64289 Darmstadt, Germany.
V.M. Shabaev. Department of Physics, St. Petersburg State University, Oulianovskaya 1, Petrodvorets, St. Petersburg 198504, Russia.
M. Vogel. Physics Department, Imperial College London, London, SW7 2BW, UK.

[1]This paper was presented at the International Conference on Precision Physics of Simple Atomic Systems, held at École de Physique, les Houches, France, 30 May – 4 June, 2010.
[2]Corresponding author (e-mail: D.vonLindenfels@gsi.de).

1. Introduction

Charged particles carry a magnetic dipole moment $\boldsymbol{\mu}$ proportional to their angular momentum $\boldsymbol{J}$. The quantities are related by the so-called gyromagnetic factor or (Landé) *g*-factor,

$$\frac{\boldsymbol{\mu}}{\mu_B} = g_J \cdot \frac{\boldsymbol{J}}{\hbar} \tag{1}$$

The Bohr magneton $\mu_B = \hbar e/2m$ is a measure of the charge-to-mass ratio of the electron, and Planck's constant $\hbar = h/2\pi$ is the unit of angular momentum.

Orbital angular momenta have $g_L = 1$, whereas for free Dirac particles g_J is 2. This value is modified by quantum electrodynamic (QED) effects, which have been calculated to the four-loop order [1] to be 2.002 319 304 365 6 (154) for the free electron. A measurement at Harvard University [2] yielded 2.002 319 304 361 46 (56), thus QED is one of the most precisely tested theories in physics.

The accuracy of the theoretical value is currently limited by the uncertainty of the fine-structure constant $\alpha = e^2/(4\pi\varepsilon_0\hbar c)$. This requires independent determinations of α, for instance in heavy ion experiments. The Coulomb potential of a nucleus shifts the g-factor — in the following we will refer to it only as g. For a single Dirac electron bound in the $1s_{1/2}$ and $2p_{1/2}$ state to a point-like nucleus, Breit [3] predicted,

$$g = 2 - \frac{2}{3}(\alpha Z)^2 + \cdots \tag{2}$$

and

$$g = \frac{2}{3} - \frac{1}{6}(\alpha Z)^2 + \cdots \tag{3}$$

respectively. For instance, (3) implies that α could be extracted from a bound-electron g-factor measurement [4, 5] with a relative uncertainty of

$$\frac{\delta\alpha}{\alpha} = \frac{3g}{(\alpha Z)^2}\frac{\delta g}{g} \tag{4}$$

An experimental accuracy of $\delta g/g = 7 \times 10^{-10}$ for bound-electron g-factor measurements in highly charged lead ions could lead to a relative uncertainty of 4×10^{-9} in the α determination from an idealized heavy ion experiment. This is comparable with the accuracy of the value $\alpha^{-1} = 137.035\,999\,45\,(62)$, obtained by atom recoil experiments [6]. They provide the best determination except for the extraction from measurements of the anomalous magnetic moment of the electron (the g-factor), which are about an order of magnitude more precise.

For an accurate treatment of the bound-electron g-factor, QED and nuclear effects have to be considered [7]. Nuclear structure contributions cancel to a high degree in a specific difference of the g-factors for $1s_{1/2}$ and $2p_{1/2}$ states, so that α can be extracted with the above stated accuracy, provided all other corrections are evaluated to the required level, as discussed in [8]. The application of this method is made possible by comparing bound electron g-factors in hydrogen-like and boron-like heavy ions, as for example in lead $^{208}Pb^{81+}$ and $^{208}Pb^{77+}$. Here, the interaction of multiple electrons comes into play, because in an atomic ground state with an unpaired p-electron, the lower-lying s-shells are occupied.

The sensitivity of the bound-electron g-factor to the fine-structure constant α is less pronounced in case of medium-heavy ions. Also, the cancellation method fails here, because it exploits two assumptions that are only satisfied in the case of heavy nuclei: (*i*) the electron mass is negligible compared with its potential energy close to the nucleus and (*ii*) the inter-electronic correlation effects are much weaker than the attractive central force. Altogether this results in an uncertainty $\delta\alpha/\alpha$ at least 30 times higher than what is possible for heavy ions. However, the study of g-factors in medium-Z ions, e.g., argon, has a further interesting aspect: electron-correlation corrections to the g-factor are of purely relativistic origin. So their measurement serves as a sensitive probe of relativistic electron-correlation effects in a regime where these effects are stronger than in light ions, but where higher orders in $1/Z$ are not yet suppressed by a too high nuclear charge.

We also consider the bound-electron g-factor measurement in highly charged argon as a pilot study for future HITRAP experiments with the above mentioned lead ions and $^{209}Bi^{82+}$.

2. Measurement principle

The bound electron magnetic moment precesses in the magnetic field B of the Penning trap at the Larmor frequency,

$$\omega_L = \frac{g}{2}\frac{e}{m}B \tag{5}$$

The magnetic field is calibrated by determining the cyclotron frequency of the trapped highly charged ion (with charge to mass ratio Q/M),

$$\omega_c = \frac{Q}{M}B \tag{6}$$

This is the basis of g-factor measurements in a Penning trap. The ratio of the two frequencies is independent of B, only the mass ratio of the electron and ion enters as an external parameter (the ion charge Q is assumed to be an exact multiple of the elementary charge e),

$$g = 2\frac{\omega_L}{\omega_c}\frac{m}{M}\frac{Q}{e} \tag{7}$$

Using this principle, bound-electron g-factors of hydrogen-like carbon and oxygen have also been measured with high accuracy [4, 9, 10].

2.1 Laser-microwave double-resonance spectroscopy

One way to measure the Larmor frequency is by using double-resonance spectroscopy. Its application to hyperfine transitions in heavy highly charged ions was proposed in [11]. Here we apply it to a fine-structure transition in a medium-heavy highly charged system.

Boron-like ions have one valence electron in the 2p shell. The splitting of the two fine-structure levels $2P_{1/2}$ and $2P_{3/2}$ scales with the nuclear charge as Z^4. In the case of boron-like $^{40}Ar^{13+}$, the magnetic dipole transition between the levels can be excited with laser radiation at about $\lambda = 441$ nm [12]. The magnetic field of 7 T in the Penning trap leads to further splitting into Zeeman sublevels with a spacing of $\omega_{MW1} = 2\pi \times 65$ GHz in the $2P_{1/2}$ state and $\omega_{MW2} = 2\pi \times 130$ GHz in the $2P_{3/2}$ state (see Fig. 1). A laser at frequency ω_1 resonantly depopulates the lowest Zeeman sub-state $|J, m_J\rangle = |1/2, -1/2\rangle$ by optical pumping. Then a closed cycle between extreme sublevels $|1/2, +1/2\rangle$ and $|3/2, +3/2\rangle$ is driven at the laser frequency ω_2.

In general, the state-selective excitation of the extreme Zeeman substate $|3/2, +3/2\rangle$ would require $\sigma+$ polarized light. Different components in an unpolarized mixture would excite transitions to different states. Here, due to the J-dependent Zeeman splitting, all visible transitions between different sublevels are separated by at least $\Delta\omega = 2\pi \times 65$ GHz, as seen in Fig. 2. This is much larger than the laser linewidth, the spacing of Doppler side bands, or the natural linewidth. If the ions are irradiated with unpolarized light, the suitable polarization component is

Fig. 1. Spectroscopy on the $2^2P_{1/2}-2^2P_{3/2}$ fine-structure transition in a boron-like argon ion with Zeeman effect. The level scheme (not to scale) and measurement principle for the double-resonance technique are shown. Solid arrows indicate excitation by laser and microwave photons [11].

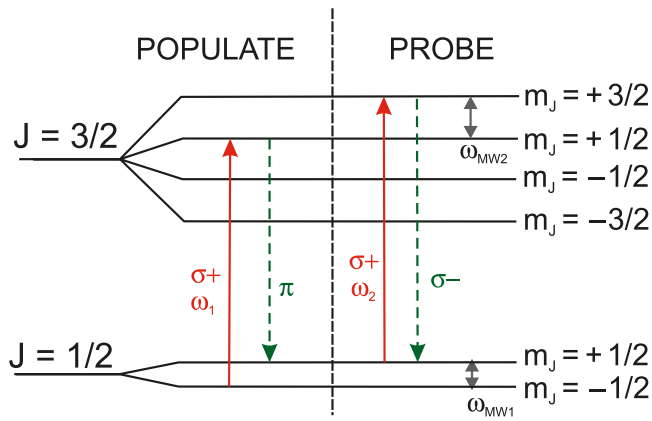

Fig. 2. Line shape with magnetic field (4 peaks, only circular polarization) and without field (single peak). ν_0 is the field-free fine-structure transition frequency.

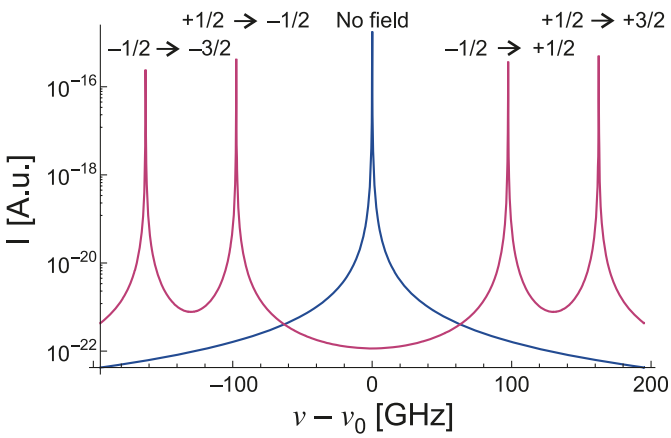

absorbed — other components are far off-resonant from their respective transition and have no effect.

Once the laser has been tuned to the resonance frequency ω_2, it remains there and repeatedly excites the $|3/2,+3/2\rangle$ state, which decays back to $|1/2,+1/2\rangle$. Then, tunable microwave radiation is shined to induce the transition from $|1/2,+1/2\rangle$ to the neighboring Zeeman sublevel $|1/2,-1/2\rangle$. The spontaneous decay of the state $|1/2,+1/2\rangle$ is practically impossible on an experimental time scale. When the microwave frequency is scanned and comes into resonance with the Larmor frequency of the ions in the magnetic field, population is transferred to the $|1/2,-1/2\rangle$ level, in which the laser radiation cannot be absorbed. This results in a minimum of the observed fluorescence intensity. Thus, the visible fluorescence serves as a probe for the population of the $J=1/2$ sublevels, indicating resonance of the microwave radiation to the Larmor frequency. This resonance frequency, together with the cyclotron frquency ω_c, yields the g-factor (see (7) above).

The lifetime of the upper fine-structure level in Ar^{13+} is 9.6 ms [13], which corresponds to a saturation intensity of approximately 20 nWcm^{-2}. Matching the unpolarized laser radiation with 1 MHz linewidth to the narrow transition makes a power density of 6 mWcm^{-2} necessary. An ensemble of about 10^5 trapped ions will cover a projected area of roughly 0.1 cm^2, requiring an estimated laser power of 0.6 mW. As a fluorescence signal, 20 counts per second can be expected on a channel photomultiplier detector (CPM), taking into account limited solid angle, transmission losses, and the detector quantum efficiency. The laser will be pulsed with a duration comparable with the upper state's lifetime. During illumination, the detector is in a blind mode. Background light by photons scattered in the trap dies out after some microseconds and will not disturb when the CPM is in its sensitive mode.

2.2. Cyclotron frequency

The measurement of the cyclotron frequency exploits basic properties of Penning traps. The strong homogeneous magnetic field confines charged particles radially. A static electric quadrupole field assures confinement in the axial direction. Stored ions perform three independent motions in such a field configuration, characterized by the reduced cyclotron frequency ω_+, the axial frequency ω_z, and the magnetron frequency ω_- [14]. A moving charge induces image currents, which are resonantly picked up in a tuned circuit and amplified at liquid helium temperature. From the measured frequencies, the free cyclotron frequency is obtained by means of the invariance theorem $\omega_c^2=\omega_z^2+\omega_+^2+\omega_-^2$ [15].

Space-charge effects would corrupt the accuracy that can be reached in a dedicated precision trap. For this reason, the determination of motional frequencies requires the reduction to a single particle. Transporting the ions between the precision trap and a reservoir trap will allow to switch quickly between laser-microwave spectroscopy and cyclotron frequency measurement, thus minimizing the uncertainty due to a magnetic field drift.

3. Implementation with medium-heavy ions

The desired particles are created from argon gas by electron-impact ionization within the trap. Therefore, a gas valve with the following properties is required. It should separate the cryogenic vacuum in a trap chamber from a room temperature, low-pressure tube attached to a gas bottle. Due to the proximity to the trapping region, the valve is situated in a strong magnetic field and has to be operable at cryogenic temperature with remote control. To our knowledge, no such valve is commercially available. Here we describe a solution that we have developed recently, modifying the idea of a cryogenic cell, and operated at JINR Dubna [16]. It comprises no moving parts but makes use of varying temperatures. Before going into detail, we give a short overview of the general setup, as is depicted in Fig. 3.

The experiment will be performed in a Penning trap assembly consisting of a creation trap, transport electrodes, and a spectroscopy trap. The first serves for ion production, intermediate storage (reservoir trap), or capturing ions coming from the HITRAP beamline at a later stage. The precision measurements of Larmor and motional frequencies takes place in the last. This trap has nearly the same harmonic electric potential as a closed compensated cylindrical Penning trap [17, 18], but it is open on one side. The miss-

Fig. 3. The experimental setup and detail: adsorption valve with resistor case and copper wire mounted. Both are viewed in vertical section.

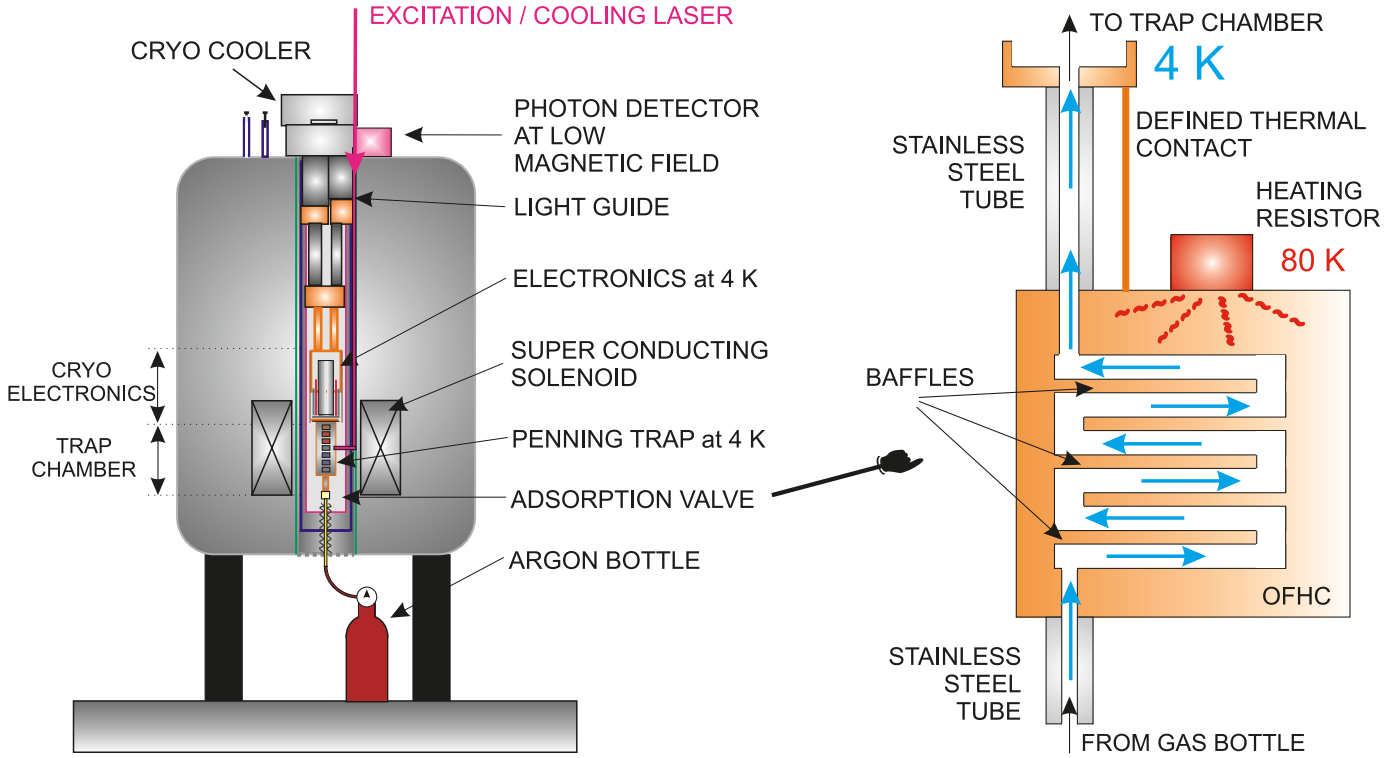

ing end cap is simulated by further electrodes to restore the harmonicity of the trapping potential. Some of them are called anti-electrodes, because they are biased with the opposite voltages of the ring and compensation electrodes. [3] Ions can easily be loaded into this half-open trap from the creation trap on the one side, and there is optical access with large solid angle for spectroscopy experiments on the other side (see Fig. 4). The electrodes are contained in an ultra-high vacuum chamber. Together with resonator coils, amplifiers, lenses, and a multi-fiber light guide, the chamber is suspended from a pulse-tube cooler in the evacuated (warm) bore of a superconducting magnet. The cooler works with two stages: The 4 K stage is connected to the trap vacuum chamber via OFHC copper rods, whereas a surrounding aluminum radiation shield is cooled to 45 K.

On the lower side, the chamber is connected to the cryogenic gas valve, through which it will be pre-pumped and, after cool-down, loaded with controlled amounts of gas for ion production. The gas valve is constructed in the following way. A narrow stainless steel tube below the vacuum chamber is followed by an oven, acylindrical copper box, partially divided by several baffles, which has a heating resistor attached (see Fig. 3). A thin OFHC copper wire enhances thermal contact between the trap chamber at 4 K and the oven in the cold (i.e., "closed" mode), ensuring a temperature of about 6 K at the oven. We chose this design for the following reason. Thermal conductivity in stainless steel is roughly proportional to the temperature in the range below 100 K, whereas in OHFC copper it follows a $1/T^2$ law between 20 and 80 K [19]. We could design a connection entirely made from stainless steel for the cold mode to have

Fig. 4. Drawing of the spectroscopy trap with a schematic view of ions and photons.

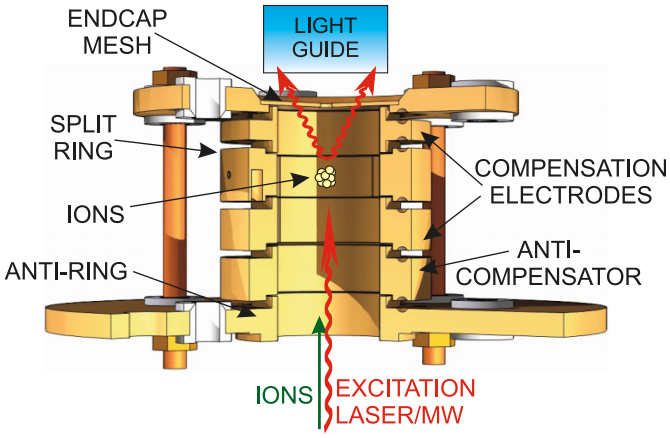

the same effect as the wire (temperature difference of only 2 K at 5 mW heat flow), but then it would cause five times more heat load in the warm (i.e., "open" mode), compared with the wire (100 mW). If on the other hand we used a copper tube, the same specification would restrict it either to be unrealistically thin or undesirably long. The system is continued by a stainless steel tube, leading out of the magnet bore, and thermally connected to the 45 K radiation shield at an intermediate point.

This valve works as follows. Atoms coming into the oven have to hit the surface many times to travel through. In the cold mode, they will most probably stick to a wall, so the box acts like a closed valve and continuously pumps resid-

[3] A detailed description of the design will be published in Rev. Sci. Instrum.

ual gas entering from the warm tube. When heated to about 80 K, two mechanisms occur: first, argon sublimes and the walls release adsorbed matter; second, the sticking probability decreases, so that the valve is in the open mode. By changing the operating parameters, such as pressure on the warm side, temperature of the box, heating time, etc., we will be able to adjust the optimum amount of gas injected into the trap chamber for ion production. Simulations and tests are pending to learn more about the gas flow through the valve. We will take into account the reproducibility, because the buildup of an argon layer on the cold surface can cause history effects.

For atoms in the trap chamber, there are two competing loss processes, adsorption to the cold walls on the one hand and ionization by electrons from a field-emission source on the other [20]. A quantitative analysis shows that even with a 10 nA electron current at an energy of 85 eV, we can expect to produce 10^5 Ar^+ ions without covering the electrodes with an argon layer, using 10^{14} atoms. Starting from singly charged ions, we breed Ar^{13+} with a production threshold of 686 eV. Then the ion cloud will be cooled, and few particles or the cloud as a whole can be transferred to the spectroscopy trap. As we have mentioned before, the magnetic field will be calibrated by the determination of the cyclotron frequency of a single ion. For this purpose, only a small fraction of the cloud is brought into the spectroscopy trap. There, the potential barrier is lowered until a single particle is left. Immediately after the cyclotron frequency measurement, the remaining ions are loaded from the reservoir for the spectroscopy experiment. Then the cloud is shifted back to the reservoir and a new cycle begins.

4. Outlook on the HITRAP project

The HITRAP facility at GSI aims to deliver a 10^5 heavy highly charged ions, cooled to liquid helium temperature, every ten seconds. Then, atomic systems with few electrons in extremely high electric and magnetic fields close to the nucleus can be investigated with high-precision ion trap experiments and collision experiments.

After testing the above described setup and techniques in off-line studies with medium-heavy ions, the g-factor experiment will use the heavy ion beam from HITRAP [21]. In particular, a double-resonance spectroscopy experiment with hydrogen-like bismuth $^{209}Bi^{82+}$ is foreseen. The nuclear spin of $I=9/2$ interacts with the electron and splits the ground state into hyperfine-structure levels with $F=4$ and 5. From g-factor measurements in both levels, electronic and nuclear moments can be disentangled [11]. The quantity g_J probes for bound-state QED, whereas the nuclear g-factor g_I, measured without diamagnetic shielding, is a benchmark for nuclear models as well as for the shielding effect itself.

5. Summary

We have recalled the idea of g-factor measurements in Penning traps in general as well as the double-resonance technique in particular. This method will be applied to forbidden transitions in the 2^2P fine-structure doublet of boron-like ions. We have described the design and working principle of a cryogenic adsorption valve. This development is an important step towards the trapping of argon ions.

Precision experiments with heavy and medium-heavy ions at HITRAP will allow for tests of QED calculations in the regime of strong fields with unprecedented accuracy. Further goals are the investigation of relativistic electron correlation effects and the determination of fundamental constants such as α. This would also increase the significance of QED tests by measurements of the free electron g-factor.

Acknowledgments

We thank K. Blaum and his group as well as Z. Andjelcovic for their support. Our colleagues, N. Bönsch, T. Dettinger, M. Eck, R. Erlenbach, E. Kammer, M. Müller, D. Racano, R. Reiter, M. Romig, and E. Wagner, deserve recognition for their excellent technological work and their consultation.We acknowledge the fruitful exchange with E.E. Donets and V.B. Shutov from JINR Dubna. Nicolas Winckler has translated the abstract into French. Our work was supported by Helmholtzgemeinschaft, Deutsche Forschungsgemeinschaft, the German Bundesministerium für Bildung und Forschung, and IMPRS school for Quantum Dynamics in Heidelberg.

References

1. T. Aoyama, M. Hayakawa, T. Kinoshita, and M. Nio. Phys. Rev. Lett. **99**, 110406 (2007). doi:10.1103/PhysRevLett.99.110406. PMID:17930419.
2. D. Hanneke, S. Fogwell, and G. Gabrielse. Phys. Rev. Lett. **100**, 120801 (2008). doi:10.1103/PhysRevLett.100.120801. PMID:18517850.
3. G. Breit. Nature, **122**, 649 (1928). doi:10.1038/122649a0.
4. M. Vogel. Contemp. Phys. **50**, 437 (2009). doi:10.1080/00107510902765239.
5. T. Beier, S. Djekic, H. Häffner, P. Indelicato, H.-J. Kluge, W. Quint, V.M. Shabaqev, J. Verdú, T. Valenzuela, G. Werth, and V.A. Yerokhin. Nucl. Instrum. Methods Phys. Res., Sect. B, **205**, 15 (2003). doi:10.1016/S0168-583X(02)01968-7.
6. M. Cadoret, E. de Mirandes, P. Cladé, S. Guellati-Khélifa, C. Schwob, F. Nez, L. Julien, and F. Biraben. Phys. Rev. Lett. **101**, 230801 (2008). doi:10.1103/PhysRevLett.101.230801. PMID:19113536.
7. W. Quint. Phys. Scr. T, **59**, 203 (1995). doi:10.1088/0031-8949/1995/T59/026.
8. V.M. Shabaev, D.A. Glazov, N.S. Oreshkina, A.V. Volotka, G. Plunien, H.-J. Kluge, and W. Quint. Phys. Rev. Lett. **96**, 253002 (2006). doi:10.1103/PhysRevLett.96.253002. PMID:16907301.
9. H. Häffner, T. Beier, N. Hermanspahn, H.-J. Kluge, W. Quint, S. Stahl, J. Verdú, and G. Werth. Phys. Rev. Lett. **85**, 5308 (2000). doi:10.1103/PhysRevLett.85.5308. PMID:11135983.
10. J. Verdú, S. Djekić, S. Stahl, T. Valenzuela, M. Vogel, G. Werth, T. Beier, H.-J. Kluge, and W. Quint. Phys. Rev. Lett. **92**, 093002 (2004). doi:10.1103/PhysRevLett.92.093002. PMID:15089462.
11. W. Quint, D.L. Moskovkhin, V.M. Shavbaev, and M. Vogel. Phys. Rev. A, **78**, 032517 (2008). doi:10.1103/PhysRevA.78.032517.
12. I. Draganić, J.R. Crespo López-Urrutia, R. DuBois, S. Fritzsche, V.M. Shabaev, R.S. Orts, I.I. Tupitsyn, Y. Zou, and J. Ullrich. Phys. Rev. Lett. **91**, 183001 (2003). doi:10.1103/PhysRevLett.91.183001. PMID:14611279.

13. A. Lapierre, U.D. Jentschura, J.R. Crespo López-Urrutia, J. Braun, G. Brenner, H. Bruhns, D. Fischer, A.J. González Martínez, Z. Harman, W.R. Johnson, C.H. Keitel, V. Mironov, C.J. Osborne, G. Sikler, R. Soria Orts, V. Shabaev, H. Tawara, I.I. Tupitsyn, J. Ullrich, and A. Volotka. Phys. Rev. Lett. **95**, 183001 (2005). doi:10.1103/PhysRevLett.95.183001. PMID:16383899.
14. F.G. Major, V.N. Gheorghe, and G. Werth. Charged particle traps. Springer, Heidelberg, Germany. 2005.
15. L.S. Brown and G. Gabrielse. Phys. Rev. A, **25**, 2423 (1982). doi:10.1103/PhysRevA.25.2423.
16. D.E. Donets, E.D. Donets, E.E. Donets, V.V. Salnikov, V.B. Shutov, and E.M. Syresin. Rev. Sci. Instrum. **80**, 063304 (2009). doi:10.1063/1.3152336. PMID:19566200.
17. G. Gabrielse and F.C. Mackintosh. Int. J. Mass Spectrom. Ion Process. **57**, 1 (1984). doi:10.1016/0168-1176(84)85061-2.
18. G. Gabrielse, L. Haarsma, and S.L. Rolston. Int. J. Mass Spectrom. Ion Process. **88**, 319 (1989). doi:10.1016/0168-1176(89)85027-X.
19. M. Schwarz. Ph.D. Thesis. Universität (TH) Karlsruhe, Germany. 2009.
20. M. Vogel, J. Alonso, S. Djekic, H.-J. Kluge, W. Quint, S. Stahl, J.L. Verdú, and G. Werth. Nucl. Instrum. Methods Phys. Res., Sect. B, **235**, 7 (2005). doi:10.1016/j.nimb.2005.03.136.
21. M. Vogel, J. Alonso, K. Blaum, W. Quint, B. Schabinger, S. Sturm, J. Verdú, A. Wagner, and G. Werth. Eur. Phys. J. Spec. Top. **163**, 113 (2008). doi:10.1140/epjst/e2008-00814-8.